

Bond and ductility: A theoretical study on the impact of construction details – part 2: Structure-specific features

Daia Zwicky*

*University of Applied Sciences Western Switzerland, College of Engineering and Architecture of Fribourg,
CH-1705 Fribourg, Switzerland*

(Received October 8, 2012, Revised April 20, 2013, Accepted June 7, 2013)

Abstract. The first part of this two-part paper discussed basic considerations on bond strength and its effect on strain localization and plastic deformation capacity of cracked structural concrete, and analytically evaluated the impacts of the hardening behavior of reinforcing steel and concrete quality on the basis of the Tension Chord Model. This second part assesses the impacts of the most frequently encountered construction details of existing concrete structures which may not satisfy current design code requirements: bar ribbing, bar spacing, and concrete cover thickness. It further evaluates the impacts of the additional structure-specific features bar diameter and crack spacing. It concludes with some considerations on the application of the findings in practice and an outlook on future research needs.

Keywords: analytical approach; assessment; anchorage; bond; codes; constitutive models; detailing; plasticity; reinforcing bars

- Continued from part 1 in Vol. 1, No. 1 -

3. Impact of construction details on bond and ductility

Code directives on detailing refer to positioning of reinforcement, concrete cover, bar spacing and bar ribbing (SIA 262 2003, Model Code 2010b). However, bond strength is also affected by further structure-specific features such as bar diameter and crack spacing. Their impacts are analyzed in more detail in Section 4.

3.1 Concrete cover thickness

The transfer of bond stresses along a reinforcing bar to the surrounding concrete demands for a tension ring around the bar (Tepfers 1973). This ring is loaded by an inner pressure from the radial diffusion of bond stresses, a.k.a wedge action. If the strength of the tension ring is reached, longitudinal cracks form along the bar, i.e., splitting. Yet, compatibility requires a second failure surface, i.e., at least a second longitudinal crack. Consequently, bond stresses can be further increased after first longitudinal cracking. Bond failure is attained by spalling of the concrete

*Corresponding author, Professor, E-mail: daia.zwicky@hefr.ch

cover, usually without further sign prior to failure, or by pull-out failure of the reinforcing bar. More detailed information on the local bond behavior and influencing parameters on concrete splitting can also be found in fib (2000), for example.

Since “brittle” tensile failure of the concrete cover with thickness c is involved in the bond transfer mechanism, crack softening plays an important role and demands considering fracture mechanical approaches. Doing so, it can be shown that the concrete cover thickness c and the bar diameter \varnothing have an important influence on bond strength (Elfgren *et al.* 1995, based on Noghabai 1995). The Model Code (2010a), for example, considers these influences by bond strength reduction factors for concrete cover thicknesses $\varnothing/2 \leq c \leq 3\varnothing$ and bar diameters $\varnothing > 25$ mm.

In older concrete structures, little concrete cover thickness has often already been planned, assuming that it would not contribute to the load-bearing behavior in the cracked state and not being aware of its function for protecting the reinforcement against corrosion. Additionally, little attention during execution was frequently paid to respecting the planned concrete cover thickness, resulting in further reduced thicknesses. For new structures, minimum thicknesses of concrete cover c are usually required, e.g., $c \geq \varnothing$ in SIA 262 (2003) and Model Code (2010a). Both codes, however, also indicate that concrete cover thickness shall be chosen with regard to concreting, e.g., greater than the maximum grain size of the aggregate plus an eventual allowance for tolerances. To be consistent with the prescriptions for new structures (SIA 262 2003), the code SIA 269/2 (2011) therefore focuses on concrete cover thicknesses $c \leq \varnothing$.

If the concrete cover is too thin, the tension ring around the bar mentioned above can only cover a limited space. Consequently, transferable bond stress is reduced. The prescriptions in SIA 269/2 (2011) were developed on the basis of the bond model proposed by Schenkel (1998) who derived transferable bond stresses based on the equilibrium of a rigid rupture cone representing failure of the longitudinally split concrete cover (Fig. 6). The transferable bond stress is determined as a function of the bar ribbing geometry, the concrete tensile strength, the failure cone geometry (inclination γ) and in particular, of the concrete cover thickness c . In tests, values of $\gamma = 25^\circ$ to 40° are typically found.

A conservative simplification of the expressions derived by Schenkel (1998) results in a transferable bond stress equal to the concrete tensile strength for vanishing concrete cover thickness, i.e., $\tau_b = f_{ct}$ for $c = 0$. This value corresponds to 50% of the value considered in the Tension Chord Model prior to yielding (Zwicky 2013). The bond model (Schenkel 1998) also confirms that a linear effect of the relative concrete cover c/\varnothing on bond strength may be assumed, as already proposed by Tepfers (1973, 1979) and as also observed experimentally (Darwin *et al.* 1992). The Model Code (2010a) considers a non-linear relationship for the impact of the relative

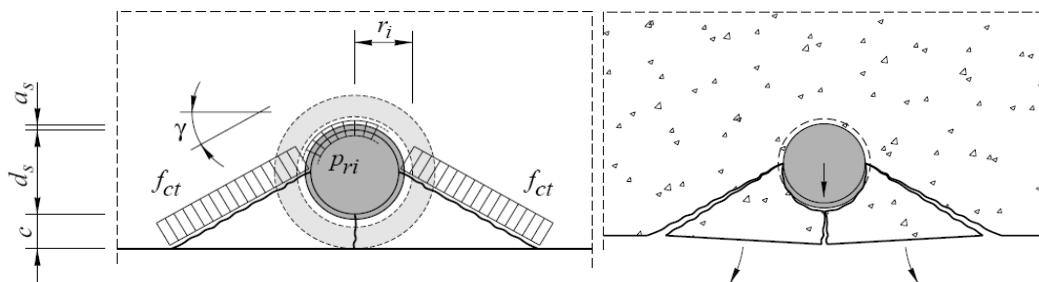


Fig. 6 Bond model for splitting failure of concrete cover (Schenkel 1998)

concrete cover c/\varnothing . SIA 269/2 (2011) only states that the bond strength is reduced to half of its value for $c = 0$ and that linear interpolation may be applied for $c \leq \varnothing$. This is interpreted here as a bond strength reduction factor $k_{b,c}$

$$k_{b,c} = 0.5 + 0.5c/\varnothing \leq 1 \quad (5)$$

Fig. 7 shows the impacts of relative concrete cover thickness c/\varnothing on strain localization. In the determination of average steel strains, see annex B in Zwicky (2013), it is assumed that the ratio τ_{b1}/τ_{b2} of Eq. (4) in Zwicky (2013) remains constant at $\tau_{b1}/\tau_{b2} = 2$. The strength reduction for bond stress level τ_{b1} is determined with Eq. (5). Remember that the bond strengths of Eq. (4) were calibrated for $c \geq \varnothing$.

There is a considerable influence on strain localization, in particular for $c/\varnothing < \text{ca. } 0.5$, and its impact is more pronounced in the hardening domain of hot-rolled steel than of cold-worked steel. Table 4 summarizes the results for strain localization factors and maximum plastic deformation capacities, also in comparison to the reference case (Section 2.4.1 in Zwicky 2013). The plastic deformation capacity is basically independent of the hardening behavior of the reinforcing steel.

The rather high increase of plastic deformation capacity with decreasing concrete cover thickness is crucially related to the assumed value of bond stress ratio τ_{b1}/τ_{b2} before and after the onset of yielding, Eq. (4) in Zwicky (2013). With this background, the impact of other ratios τ_{b1}/τ_{b2} on the global deformation behavior of a crack element is analyzed in Fig. 8. The transferable bond

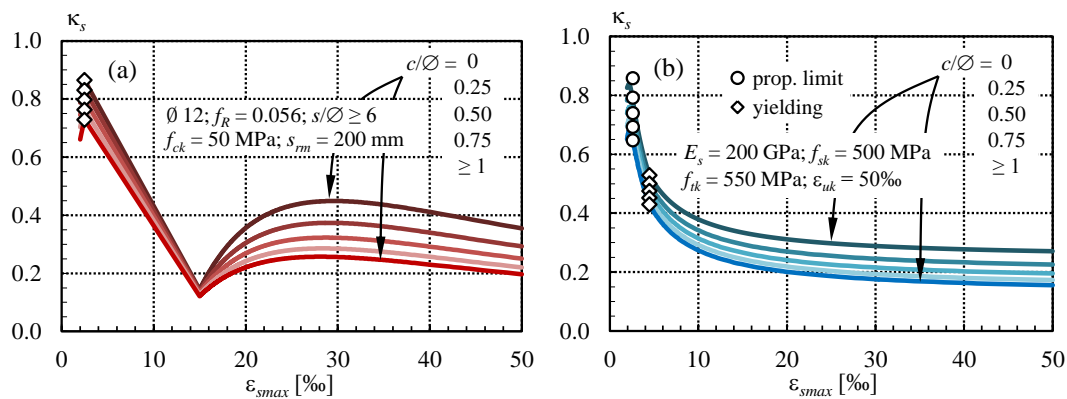


Fig. 7 Impact of relative concrete cover thickness c/\varnothing on strain localization for (a) hot-rolled steel and (b) cold-worked steel

Table 4 Impact of relative concrete cover c/\varnothing on strain localization factors and plastic deformation capacity

c/\varnothing	0			0.25			0.5			0.75			≥ 1			
Steel	HR	CW _y	CW _p	HR	CW _y	CW _p	HR	CW _y	CW _p	HR	CW _y	CW _p	HR	CW _y	CW _p	
κ_{sy}	0.86	0.53	0.86	0.83	0.50	0.79	0.80	0.47	0.74	0.76	0.45	0.69	0.73	0.43	0.65	
κ_{su}	0.35	0.27	0.29	0.23	0.25	0.25	0.20	0.22	0.17	0.20	0.16					
$\Delta\varepsilon_{pl}$	%	15.56	11.16	11.31	12.55	9.04	9.23	10.54	7.62	7.83	9.11	6.60	6.83	8.03	5.84	6.09
	rel.	194%	191%	186%	156%	155%	152%	131%	130%	129%	113%	113%	112%		100%	

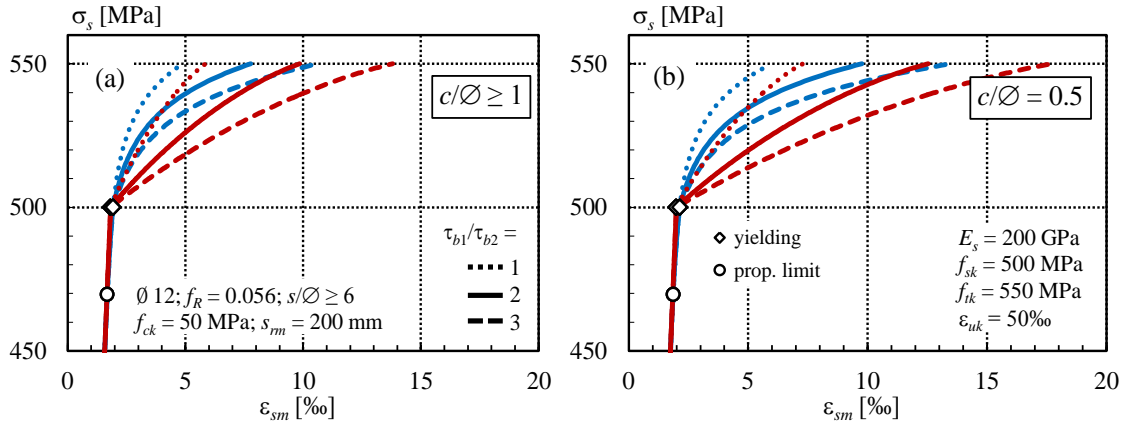


Fig. 8 Impact of τ_{b1}/τ_{b2} ratio on average strains in a crack element for (a) $c/\varnothing \geq 1$ and (b) $c/\varnothing = 0.5$ for hot-rolled steel (red lines) and cold-worked steel (blue lines)

stress decreases at splitting but the latter has less impact on residual bond strength being primarily provided by friction between reinforcing steel and concrete (fib 2000). It may therefore be expected that the bond strength ratio τ_{b1}/τ_{b2} for reduced concrete cover thickness rather increases (Engström *et al.* 1998, Huang *et al.* 1996) to values above the reference level for tension chords with sufficient concrete cover. Note, however, that the absolute levels of bond strength decrease. Nevertheless, for reasons of comparison, a ratio $\tau_{b1}/\tau_{b2} = 1$ is also considered in Fig. 8. Eq. (5) is used to determine the reduction of τ_{b1} .

The graphs in Fig. 8 reveal that the assumption for the bond strength level after the onset of yielding or the bond strength ratio, respectively, has an important impact. For the chosen values of τ_{b1}/τ_{b2} , the total plastic deformation capacity varies within limits of approx. $\pm 50\%$ of the reference case (Section 2.4.1 in Zwicky 2013), independently of the hardening behavior of the reinforcing steel. For $c = \varnothing/2$, the plastic deformation capacity increases to roughly 130% of the capacity for $c/\varnothing \geq 1$. Unfortunately, no experimental data is available on this issue, i.e., bond tests for the combination of plastic steel strains and very small concrete cover (i.e. $c < \varnothing$) though it certainly deserves experimental investigations.

Experimental results show that a substantial reduction of bond strength also has to be expected if reinforcing bars are located close to section corners (Huang *et al.* 1996). The bond model by Schenkel (1998) also allows treating these cases where the failure cone is cut in by the lateral surface (Fig. 6). For a bond behavior independent of the lateral surface, a minimum ratio of two orthogonal concrete covers c and c_{lat} must be available. Assuming a relatively conservative failure cone geometry with $\tan \gamma = 0.5$ (i.e., $\gamma \approx 27^\circ$) and $c = \varnothing$ results in the expression provided in SIA 269/2 (2011)

$$k_{b,c,lat} = \frac{1}{2} + \frac{c_{lat}/c}{4 + 2\varnothing/c} \leq 1 \quad \text{if } c_{lat} \leq 3c \quad (6)$$

The consequences of Eq. (6) on strain localization and plastic deformation capacity are not analyzed here in detail.

3.2 Bar spacing

Spacing s of reinforcing bars may also have an influence on bond strength: if the bars are rather close to each other, the splitting failure cones of adjacent bars (Fig. 6) may intersect, consequently resulting in lower bond strength. For a bar spacing less than a critical bar spacing s_{crit} , the bond behavior of the single bars is not independent anymore and the concrete cover will spall off on a larger surface, thus also requiring the consideration of approaches based on fracture mechanics (also see Section 3.1).

The value of the critical bar spacing s_{crit} depends on the concrete cover thickness c and the inclination γ of the failure cones (Fig. 6). Assuming $c = \emptyset$ and $\gamma = 30^\circ$, tending to be a conservative value (Section 3.1), in the rigid-body failure cone approach proposed by Schenkel (1998) results in $s_{crit} \geq 6\emptyset$, being the limit considered in the directives of SIA 269/2 (2011) for an independent bond behavior of closely spaced bars. The Model Code (2010a) requires $11\emptyset$ for $c = \emptyset$.

If the present bar spacing s is below the critical bar spacing s_{crit} , a linear reduction of bond strength may be considered (Schenkel 1998), with vanishing bond strength for $s = \emptyset$, i.e., adjacent bars, as also confirmed experimentally (Darwin *et al.* 1992). The impact of bar spacing s on bond strength is analyzed here by the means of an associated bond strength reduction factor $k_{b,s}$

$$k_{b,s} = \frac{s - \emptyset}{5\emptyset} \leq 1 \quad (7)$$

Fig. 9 shows the impact of bar spacing on strain localization, presuming again that the τ_{b1}/τ_{b2} ratio, Eq. (4) in Zwicky (2013), remains constant at $\tau_{b1}/\tau_{b2} = 2$. The strength reduction for bond stress level τ_{b1} is determined with Eq. (7).

The bar spacing has a tremendous effect on strain localization, above all in the hardening domain and more pronounced for hot-rolled than for cold-worked steel. Before onset of yielding, the influence of bar spacing is less important. Table 5 summarizes the results, also in comparison to the reference case (Section 2.4.1 in Zwicky 2013). Hardening characteristic and bar spacing have a noticeable interaction on plastic deformation capacity, particularly for very small bar spacing.

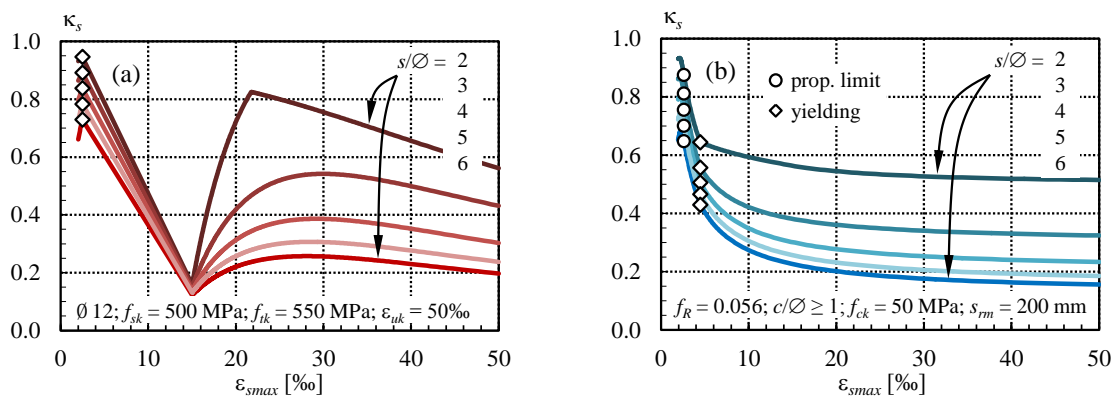


Fig. 9 Impact of relative bar spacing s/\emptyset on strain localization for (a) hot-rolled steel and (b) cold-worked steel

Table 5 Impact of relative bar spacing s/\varnothing on strain localization factors and plastic deformation capacity

c/\varnothing	2			3			4			5			6			
Steel	HR	CW _y	CW _p	HR	CW _y	CW _p	HR	CW _y	CW _p	HR	CW _y	CW _p	HR	CW _y	CW _p	
κ_{sy}	0.95	0.64	0.88	0.89	0.56	0.81	0.84	0.51	0.75	0.78	0.47	0.70	0.73	0.43	0.65	
κ_{su}	0.56	0.51	0.43	0.32	0.30	0.23	0.24	0.19	0.20	0.16						
$\Delta \varepsilon_{pl}$	%	25.72	22.84	23.45	19.33	13.70	14.09	13.05	9.40	9.71	9.91	7.18	7.45	8.03	5.84	6.09
rel.	320%	391%	385%	241%	235%	231%	163%	161%	160%	123%	123%	122%			100%	

The high increase of plastic deformation capacity with decreasing bar spacing is crucially related to the assumption of the bond stress ratio before and after the onset of yielding. It can be expected that the impact of other τ_{b1}/τ_{b2} ratios is similar to the one from concrete cover thickness (Fig. 8) and would thus certainly deserve more detailed experimental investigations as well.

3.3 Bar ribbing

After attaining a very small contribution from adhesion between concrete and steel, bond stresses between regularly ribbed reinforcing bars and surrounding concrete are essentially transferred by interlocking of the ribs on the bar with the concrete, i.e., by shear bond. However, the bond strength does not vanish for smooth bars. They also provide a certain bond strength, usually attained by pull-out failure, due to the micro-roughness of the bar skin from fabrication processes (fib 2000, Schenkel 1998). The bond strength is essentially provided by dry friction between concrete and bar, thus being additionally influenced by transverse pressure from concrete shrinkage or lateral bearing stresses, for example.

For the comparison of different ribbing geometries, reference is usually made to the relative rib area f_R proposed by Rehm (1961). This parameter describes the ratio of the rib area – projected to the bar cross-section in the case of skew ribs – to skin surface between the ribs. For conventional ribbing, this ratio roughly corresponds to the ratio of rib height to rib spacing. The relative rib area f_R of smooth bars thus amounts to $f_R = 0$.

Early research on bond behavior of reinforcing bars (Rehm 1961) already showed that the bond strength depends more or less linearly on the relative rib area f_R . For the elaboration of SIA 269/2 (2011), an approach for determining the bond strength of smooth bars in a simple way thus had to be found.

The bond strength of pre-tensioning wires and strands with smooth to indented surfaces is treated representatively in Zwicky (2002). Average bond strengths are derived, applying the local bond stress-slip relationship $\tau_b = C \cdot \delta^N$ (Noakowski 1998). The values for the constants C and N , depending on the surface characteristics and position of the reinforcing bars during concreting, are taken from literature (Noakowski 1988, Bruggeling 1991) for different levels of relative rib area, also see Section 4.1. A linear effect of relative rib area f_R on the bond strength is proposed. The adjustment of the proposals in Zwicky (2002) to the current design concept and design values of SIA 262 (2003) is expressed in SIA 269/2 (2011) as a reduction factor $k_{b,fR}$ to be applied to the bond strength of regularly ribbed reinforcing bars

$$k_{b,fR} = 0.55 + 8f_R \leq 1 \tag{8}$$

where f_R = relative rib area. The provisions of Model Code (2010a) result in a comparable bond strength reduction factor of 0.514 for plain surface bars, i.e., $f_R = 0$. For new concrete structures, $f_R \geq 0.056$ is required for $\varnothing > 12$ mm (SIA 262 2003). The coherence of SIA 269/2 (2011) with SIA 262 (2003) is thus given, at least for frequently encountered bar diameters $\varnothing > 12$ mm, since Eq. (8) results in $k_{b,fR} = 0.998 \approx 1$ for $f_R = 0.056$. Small bar diameters may have a reduced relative rib area: $f_R = 0.035$ for $\varnothing \leq 6$ mm and $f_R = 0.040$ for $6.5 \text{ mm} < \varnothing \leq 12$ mm (SIA 262 2003).

Fig. 10 compares average strains in a crack element for varying relative rib area f_R , again presuming that the ratio τ_{b1}/τ_{b2} of Eq. (4) in Zwicky (2013) remains constant at $\tau_{b1}/\tau_{b2} = 2$. The strength reduction for bond stress level τ_{b1} is determined with Eq. (8). The impact of bar ribbing on plastic deformation capacity is less pronounced than what would be expected. It only has a marked influence after onset of yielding, and it is again more pronounced for hot-rolled than for cold-worked steel.

A structure with smooth reinforcement should thus provide increased plastic deformation capacity. If no information on the bar ribbing can be drawn from the construction files or from code requirements valid at the time of construction, it is advisable to try to obtain such information from other sources, e.g., ancient product information leaflets or probing.

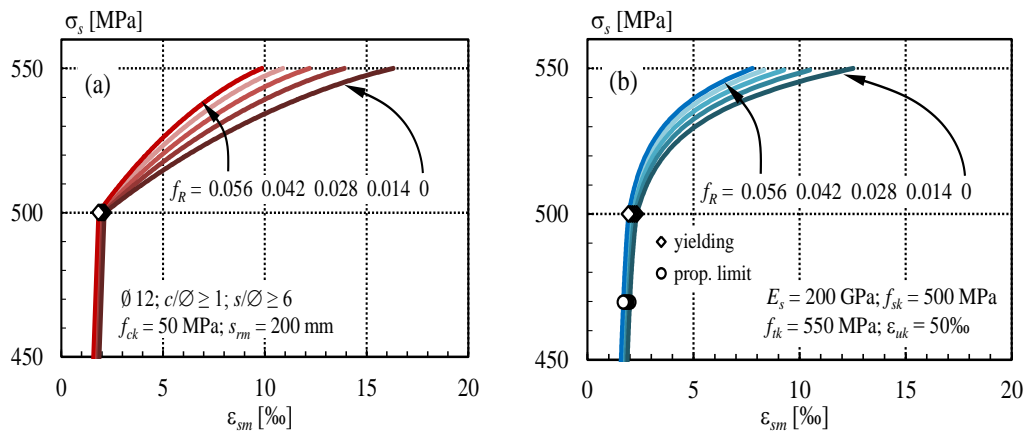


Fig. 10 Impact of bar ribbing f_R on average strains in a crack element for (a) hot-rolled steel and (b) cold-worked steel

Table 6 Impact of bar ribbing f_R on strain localization factors and plastic deformation capacity

f_R	0			0.014			0.028			0.042			0.056		
Steel	HR	CW _v	CW _p												
κ_{sy}	0.85	0.52	0.77	0.82	0.49	0.74	0.79	0.47	0.71	0.76	0.45	0.68	0.73	0.43	0.65
κ_{su}	0.33	0.25	0.28	0.28	0.22	0.24	0.19	0.22	0.17	0.20	0.17	0.20	0.20	0.16	0.16
%	14.19	10.21	10.53	11.88	8.57	8.86	10.23	7.40	7.67	9.00	6.53	6.79	8.03	5.84	6.09
$\Delta\epsilon_{pl}$ rel.	176%	174%	173%	148%	146%	145%	127%	126%	126%	112%	112%	111%	100%	100%	100%

4. Impact of further structure-specific features

4.1 Bar diameter

Codes usually limit the applicability of their directives with regard to bond strength to bar diameters relevant in practice, e.g., $\varnothing \leq 40$ mm (SIA 262 2003) or $\varnothing \leq 25$ mm (Model Code 2010a), providing bond strength values independent of the bar diameter. The same applies for the Tension Chord Model (Marti *et al.* 1998) used here, see Fig. 1 in Zwicky (2013). However, it can be shown analytically and experimentally that regularly ribbed bars of smaller diameter provide less bond strength than large bar diameters (Noghabai 1995, Sigrist 1995), in particular for $\varnothing < \text{ca. } 12$ mm, also see Fig. 11. This may also be partially related to the smaller relative rib areas of bars with smaller diameter (Section 3.3). Note, however, that the effect of bar diameter on bond strength may be inverted for smooth bars, i.e., bond strength decreases with increasing bar diameter (Bazant *et al.* 1995).

As outlined in Section 2.3 of Zwicky (2013), the bond stress level before the onset of yielding was derived in Sigrist (1995) from theoretical considerations. Based on the hypothesis that the ascending branch of the local bond stress-slip law $\tau_b = C \cdot \delta^N$ (Noakowski 1998) is valid up to steel yielding, the length of a reinforcing bar necessary for anchoring its yield force as well as an associated average bond stress τ_{bm} can be derived

$$\tau_{b1} = \tau_{bm} = \frac{1-N}{8} \left(\frac{8C}{1+N} \right)^{\frac{1}{1+N}} \left[\frac{f_y^2}{E_s} \varnothing \right]^{\frac{N}{1+N}} \quad (9)$$

where N and C are parameters reflecting the surface characteristics and position of reinforcing bars during concreting. Usually, $C = 0.42(f_{ck,cube})^{2/3}$ and $N = 0.10$ can be assumed for smooth bars (Noakowski 1988) and $C = 0.8(f_{ck})^{2/3}$ and $N = 0.15$ for regularly ribbed bars (Sigrist 1995), respectively.

Fig. 11 compares results from Eq. (9), applying the mentioned values for C and N , to the bond strength determined from Eqs. (4)₁ and (8) considering different bar ribbing and concrete compressive strengths frequently encountered in practice. A typical yield strength of $f_{sk} = 500$ MPa is considered for ribbed bars; for smooth bars, a typical value of $f_{sk} = 235$ MPa is applied (SIA

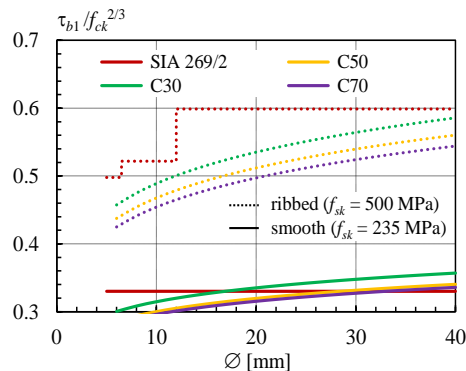


Fig. 11 Average bond strength τ_{b1} before onset of steel yielding as a function of bar diameter \varnothing

269/2 2011). $f_R = 0$ is assumed for smooth bars while the requirements of SIA 262 (2003) are considered for regularly ribbed bars (Section 3.3).

The comparison shows that the prescriptions of SIA 269/2 (2011) reasonably approach the refined solution of Eq. (9) for smooth bars and tend to be conservative for ribbed bars. An overestimation of bond strength results in more pronounced strain localization and an associated reduction in plastic deformation capacity. Also note that the bond strength according to SIA 262 (2003) for checking anchorage and lap splice lengths is reduced to a design value while plastic deformation capacity calculation should rather be performed with average material strengths.

With regard to strain localization and plastic deformation capacity, the bar diameter of a given reinforcement cross-section has a direct impact on the theoretical limits of average crack spacing, also see Section 4.2. Furthermore, the bar diameter influences the gradient of steel strains between adjacent cracks (Sigrist 1995, Alvarez 1998), hence influencing the average strain in a crack element or strain localization, respectively (annex B in Zwicky 2013). Last but not least, the bar diameter also interacts with the concrete cover thickness c if the latter has an absolute value (Section 3.1).

Fig. 12 shows strain localization factors for usual bar diameters \varnothing . It confirms the softer bond behavior for larger bar diameters: a higher value of strain localization factor corresponds to a less pronounced variation of steel strains between two cracks, i.e. a less pronounced localization of steel strains at cracks (Section 2.2.2 in Zwicky 2013). This should not surprise because the maximum steel strain at cracks depends on \varnothing^2 (for a given force in the bar) while the bond stiffness only varies linearly with the skin surface, i.e., linearly with \varnothing . The impact of bar diameter is again more marked for hot-rolled than for cold-worked steel and, in particular, for small bar diameters before and after the onset of yielding.

Table 7 summarizes the results for strain localization factors and maximum plastic deformation capacities, also in comparison to the reference case (Section 2.4.1 in Zwicky 2013). The plastic deformation capacity is almost independent of the steel hardening behavior. Cold-worked steel attains approx. 73% of the plastic deformation capacity of hot-rolled steel.

Reinforcing bars of larger diameters thus provide higher plastic deformation capacity, e.g. larger rotations in plastic hinges (Eq. (1) in Zwicky 2013), if the ultimate strain in the concrete compression zone is not governing (Sigrist 1995, Kenel 2002), see Eq. (2) in Zwicky (2013). As

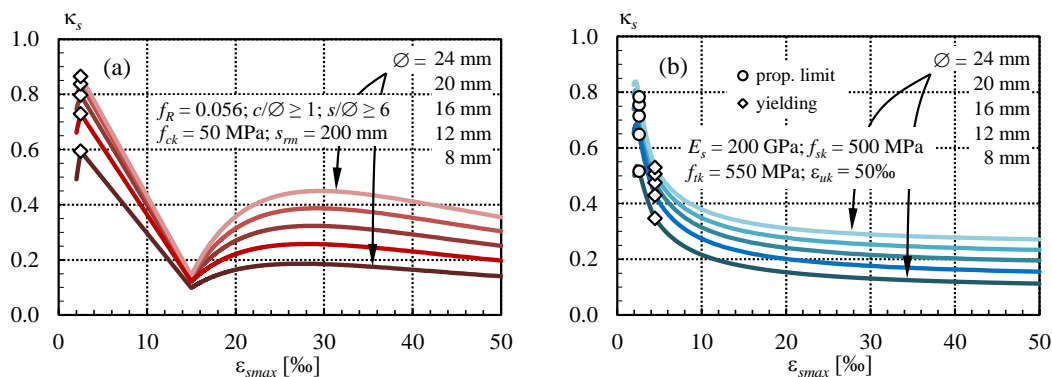


Fig. 12 Impact of bar diameter \varnothing on strain localization for (a) hot-rolled steel and (b) cold-worked steel

Table 7 Impact of bar diameter \varnothing on strain localization factors and plastic deformation capacity

\varnothing	8 mm			12 mm			16 mm			20 mm			24 mm			
	Steel	HR	CW _y	CW _p	HR	CW _y	CW _p	HR	CW _y	CW _p	HR	CW _y	CW _p	HR	CW _y	CW _p
κ_{sy}	0.59	0.35	0.52	0.73	0.43	0.65	0.80	0.48	0.71	0.84	0.51	0.76	0.86	0.53	0.78	
κ_{su}	0.14		0.11	0.20		0.16	0.25		0.20	0.30		0.23	0.36		0.27	
$\Delta\varepsilon_{pl}$	%o	5.53	4.07	4.28	8.03	5.84	6.09	10.56	7.64	7.91	13.08	9.42	9.73	15.59	11.19	11.53
	rel.	69%	70%	70%		100%		131%	130%	130%	163%	161%	160%	194%	191%	189%

shown by the numbers in Table 7, the increase in plastic deformation capacity may be rather important. Probing for present bar diameters in an existing concrete structure may therefore be advisable if no construction drawings are available; in this case, the probing must be performed anyway since it also provides the necessary information for determining structural resistances. The probing will also be beneficial for the determination of other characteristics, e.g., steel type through product identification by ribbing geometry, thickness of concrete cover etc.

4.2 Average crack spacing

The average crack spacing s_{rm} in a tension chord to be considered in the determination of plastic deformation capacity is a consequence of construction details, and thus also a structure-specific feature. On the one hand, expectable limits of average crack spacing depend on the provided reinforcement, and, on the other hand, it depends very much on the given spacing of transverse reinforcement.

Theoretical boundaries of average crack spacing s_{rm} can also be derived from the Tension Chord Model (Marti *et al.* 1998)

$$l_0 \leq s_{rm} \leq 2l_0 \quad \text{with} \quad l_0 = \frac{\varnothing f_{ct}(1-\rho)}{4\tau_{b1}\rho} = \frac{\varnothing(1-\rho)}{8\rho} \approx \frac{\varnothing}{8\rho} \quad (10)$$

where $\rho = \varnothing^2\pi/(4A_c) =$ geometrical reinforcement ratio with $\varnothing =$ bar diameter, and $A_c =$ gross concrete cross-section of the tension chord. For profiled girders, the gross concrete cross-section of the flexural tension flange can normally be considered for the determination of the geometrical reinforcement ratio. For rectangular cross-sections, other approaches should be applied, e.g., Schiessl (1989). Eq. (10) essentially differentiates between two situations: the concrete tensile strength is attained again or just not between two adjacent cracks due to the tensile stresses transferred to the concrete by bond stresses of the reinforcement.

A comparison with other proposals for the estimation of crack spacing in flexural members can be found in Kenel (2002), for example. In practice, however, cracking will usually occur at the location of transverse reinforcing bars. If an entire multiple of the transverse reinforcement spacing is found within the boundaries of Eq. (10), this is the most probable average crack spacing.

Fig. 13 therefore shows the impact of absolute values of average crack spacing s_{rm} on average

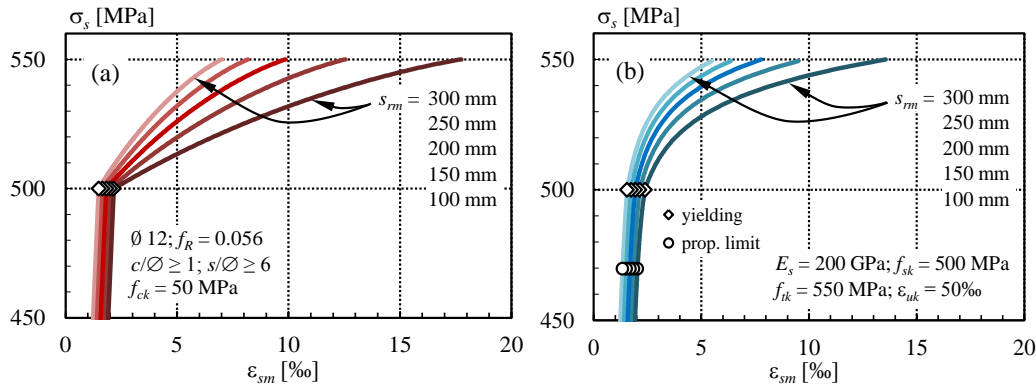


Fig. 13 Impact of average crack spacing s_{rm} on average strains in a crack element for (a) hot-rolled steel and (b) cold-worked steel

Table 8 Impact of average crack spacing s_{rm} on strain localization factors and plastic deformation capacity

s_{rm}	100 mm			150 mm			200 mm			250 mm			300 mm			
Steel	HR	CW _v	CW _p													
κ_{sy}	0.86	0.53	0.78	0.80	0.48	0.71	0.73	0.43	0.65	0.66	0.39	0.58	0.59	0.35	0.52	
κ_{su}	0.36	0.27	0.25	0.20	0.20	0.20	0.16	0.16	0.13	0.14	0.11					
$\Delta\epsilon_{pl}$	%	15.59	11.19	11.53	10.56	7.64	7.91	8.03	5.84	6.09	6.54	4.78	5.01	5.53	4.07	4.28
	rel.	194%	191%	189%	131%	130%		100%		81%	82%	82%	69%	70%	70%	

strains in a crack element, revealing a pronounced impact in the whole steel strain range. Table 8 summarizes the results for strain localization factors and maximum plastic deformation capacities, also in comparison to the reference case (Section 2.4.1 in Zwicky 2013). The plastic deformation capacity changes are essentially independent of the hardening behavior of the reinforcing steel and indicate that hardening characteristic and crack spacing have no interaction. Bars made of cold-worked reinforcing steel provide approx. 73% of the deformation capacity of bars made of hot-rolled steel.

The results confirm the well-known fact that small crack spacing is generally advantageous for the deformation behavior of structural concrete, not only at serviceability limit state but also with regard to plastic deformation capacity. Attention should therefore be given to a sound estimation of the absolute value of average crack spacing, in particular, if relatively small values of average crack spacing (approx. below 200 mm) can be expected. This will essentially be the case if the tension chord is provided with a high reinforcement ratio from bars of small diameter, see Eq. (10).

5. Conclusions

This study allows the following conclusions

- The plastic deformation capacity of structural concrete strongly depends on the hardening behavior of the reinforcement and on the bond characteristics between reinforcement and concrete. It may vary considerably as a function of further structure-specific features.

- Construction details and other structure-specific features may have a considerable effect on bond strength and, thereby, also on plastic deformation capacity. The recent Swiss code SIA 269/2 (2011) on existing concrete structures is among the first national codes addressing – in a concise, simple and appropriate way for practical application – bond strength reduction for cases where construction details do not comply with requirements for new structures (e.g., SIA 262 2003). The results presented here may help the structural engineer in practice to better estimate the impact of a specific feature on bond strength and plastic deformation capacity.
- According to the presented results, the governing structure-specific features are in decreasing order of importance: bar spacing, bar diameter, average crack spacing, concrete cover thickness, ultimate steel strain, bar ribbing and concrete quality. Bar diameter and reinforcement ratio may determine the average crack spacing.
- The simple and unified Tension Chord Model can be extended to assessing the impact of construction details on bond strength. The associated bond strength values before and after the onset of yielding should be calibrated with experimental results, gained from specimens that are reinforced with differently hardening steel and that allow attaining large plastic reinforcement strains while varying the mentioned construction details as well as the bar diameter.

Acknowledgements

Code provisions are usually not formulated by a single person. The hundreds of comments received during the consultation phase of the Swiss code SIA 269/2 (2011) on existing concrete structures allowed the author to considerably improve and condense the initial proposals. The tremendous work of all commenters as well as the very pleasant collaboration with the other individuals of the working group for the creation of the code is thankfully acknowledged.

Further Information

The following references are downloadable for free at <http://e-collection.ethbib.ethz.ch>: Alvarez, M. (1998); Kenel, A. (2002); Schenkel, M. (1998); Sigrist, V. (1995); Zwicky, D. (2002).

References

- Alvarez, M. (1998), *Einfluss des Verbundverhaltens auf das Verformungsvermögen von Stahlbeton (Influence of bond behavior on the deformation capacity of structural concrete, in German)*, Institute of Structural Engineering, **236**, Swiss Federal Institute of Technology, Zurich, Switzerland.
- Bazant, Z.P., Li, Z. and Thoma, M. (1995), “Identification of stress-slip law for bar or fiber pull-out by size effect test”, *ASCE J. Eng. Mech.*, **121**(5), 620-625.
- Bruggeling, A.S.G. (1991), *Structural Concrete – Theory and its Application*, Balkema Rotterdam.
- Darwin, D., McCabe, S.L., Idun, E.K. and Schoenekase, S.P. (1992), “Development length criteria: Bars not confined by transverse reinforcement”, *ACI Struct. J.*, **89**(6), 709-720.
- Elfgren, L., Noghabai, K., Ohlsson, U. and Olofsson, T. (1995), “Applications of fracture mechanics to anchors and bond”, *Proc. 2nd Int'l Conf. on Fracture Mechanics of Concrete Structures*, Vol. III, Aedificatio Publ., Zurich, Switzerland, 1685-1694.
- Engström, B., Magnusson, J. and Huang Z. (1998), “Pull-out bond behavior of ribbed bars in normal and high-strength concrete with various confinements”, *Bond and Development of Reinforcement: A tribute to Dr. Peter Gergely, ACI-Int. SP-180*, 215-242.

- fib (2000), “Bond mechanisms including pull-out and splitting failures”, Bond of reinforcement in concrete – state-of-the-art report, bulletin no. 10, *Int. Federation Struct. Concrete (fib)*, Lausanne, Switzerland, 1-98.
- Huang, Z., Engström, B. and Magnusson, J. (1996), *Experimental investigation of the bond and anchorage behavior of deformed bars in high strength concrete*, **95:4**, Division of Concrete Structures, Dept. of Structural Engineering, Chalmers University of Technology, Gothenburg, Sweden.
- Kenel, A. (2002), *Biegetragverhalten und Mindestbewehrung von Stahlbetonbauteilen (Bending behavior and minimum reinforcement of structural concrete elements, in German)*, **277**, Institute of Structural Engineering, Swiss Federal Institute of Technology, Zurich, Switzerland.
- Marti, P., Alvarez, M., Kaufmann, W. and Sigrist, V. (1998), “Tension chord model for structural concrete”, *Struct. Eng. Int'l.*, **8(4)**, 287-298.
- Mayer, U. (2003), *Zum Einfluss der Oberflächengestalt von Rippenstählen auf das Trag- und Verformungsverhalten von Stahlbetonbauteilen (Influence of the rib pattern of ribbed reinforcement on the structural behavior of reinforced concrete members, in German)*, **537**, Deutscher Ausschuss für Stahlbeton, Beuth Berlin, Germany.
- Model Code (2010a), *Model Code 2010 – Final draft, Vol. 1*, **65**, International Federation for Structural Concrete (fib), Lausanne, Switzerland.
- Model Code (2010b), *Model Code 2010 – Final draft, Vol. 2*, **66**, International Federation for Structural Concrete (fib), Lausanne, Switzerland.
- Noakowski, P. (1988), *Nachweisverfahren für Verankerung, Verformung, Zwangsbeanspruchung und Rissbreite (Verification procedure for anchorage, deformation, restraint loading and crack width, in German)*, **394**, Deutscher Ausschuss für Stahlbeton, Beuth Berlin, Germany.
- Noghabai, K. (1995), “Splitting of concrete covers – a fracture mechanics approach”, (Ed. Wittman, F.H.), *Proc. 2nd Int'l Conf. on Fracture Mechanics of Concrete Structures*, Vol. II, Aedificatio Publ., Zurich, Switzerland, 1575-1584.
- Rehm, G. (1961), *Über die Grundlagen des Verbunds zwischen Stahl und Beton (On the fundamentals of bond between steel and concrete, in German)*, Deutscher Ausschuss für Stahlbeton, Ernst & Sohn Berlin, **138**, Germany.
- Schenkel, M. (1998), *Zum Verbundverhalten von Bewehrung bei kleiner Betondeckung (On the bond behavior of reinforcement with small concrete cover, in German)*, **237**, Institute of Structural Engineering, Swiss Federal Institute of Technology, Zurich, Switzerland.
- Schiessl, P. (1989), “Grundlagen der Neuregelung zur Beschränkung der Rissbreite (Basics for the new directives on crack width limitation, in German)”, Erläuterungen zu DIN 1045, “Beton- und Stahlbeton – Ausgabe 07.1988”, **400**, Deutscher Ausschuss für Stahlbeton, Beuth Berlin, Germany, 157-175.
- SIA 262 (2003), *Concrete structures*, Swiss Society of Engineers and Architects (SIA), Zurich, Switzerland.
- SIA 269/2 (2011), *Existing structures – concrete structures*, Swiss Society of Engineers and Architects (SIA), Zurich, Switzerland (in German and French).
- Sigrist, V. (1995), *Zum Verformungsvermögen von Stahlbetonträgern (On the deformation capacity of reinforced concrete girders, in German)*, **210**, Institute of Structural Engineering, Swiss Federal Institute of Technology, Zurich, Switzerland.
- Tepfers, R. (1973), *A theory of bond applied to overlapped tensile reinforcement splices for deformed bars*, **73/2**, Division of Concrete Structures, Dept. of Structural Engineering, Chalmers University of Technology, Gothenburg, Sweden.
- Tepfers, R. (1979), “Cracking of concrete cover along anchored deformed reinforcing bars”, *Mag. Concrete Res.*, **31(106)**, 3-12.
- Zwicky, D. (2013), “Bond and ductility: a theoretical study on the impact of construction details – part 1: basic considerations”, *Adv. Concr. Constr.*, **1(1)**, 103-119.
- Zwicky, D. (2002), *Zur Tragfähigkeit stark vorgespannter Betonbalken (On the bearing capacity of highly prestressed concrete girders, in German)*, **275**, Institute of Structural Engineering, Swiss Federal Institute of Technology, Zurich, Switzerland.